

SRESLi: SMART RENEWABLE ENERGY STREET LIGHTING SYSTEM

SRESLi: SISTEMA DE ILUMINACIÓN VIAL INTELIGENTE CON ENERGÍA RENOVABLE

Fabiana Cañipa¹, Fabio Arnez², Omar Ormachea¹, Alex Villazón², Armando Rivero³, Gian Carlo Dozio³ and Erick Escobar¹

¹*Centro de Investigaciones Ópticas y Energías (CIOE)*

²*Centro de Investigaciones de Nuevas Tecnologías Informáticas (CINTI)*
Universidad Privada Boliviana
oormachea@upb.edu

³*Scuola Universitaria Professionale della Svizzera Italiana (SUPSI)*
(Recibido el 28 de mayo 2019, aceptado para publicación el 28 de junio 2019)

ABSTRACT

Conventional street lighting systems do not allow controlling the light intensity depending on the traffic of pedestrians or vehicles, only operate in two automatic modes (on/off) according to the availability of daylight and consume enormous amounts of electric energy. In this article, we describe the design, development and implementation of a new intelligent street lighting system that is based on LED technology, an energy-efficient embedded wireless control device (hardware) designed from scratch, and photovoltaic solar energy. The embedded device includes specialized firmware and an energy-efficient wireless communication protocol, that allows to form a network of infrared sensors to detect pedestrians and vehicles, so as to control and dim the LED luminaires. We implemented a pilot system in a back road of the campus of Universidad Privada Boliviana, in the city of Cochabamba, Bolivia, where energy consumption measurements confirm energy savings of 72.8% thanks to the developed intelligent control system.

Keywords: Street Lighting System, Photovoltaic System, Intelligent Wireless Control System, Energy Efficiency.

RESUMEN

Los sistemas convencionales de iluminación vial no permiten el control de la intensidad de luz en función del tráfico de peatones o vehículos, sólo tienen dos modos de operación automático (prendido/apagado) dependiendo de la luz del día, y consumen una gran cantidad de energía eléctrica. En este artículo se describe el diseño, desarrollo, e implementación de un nuevo sistema de iluminación vial inteligente basado en tecnología LED, un dispositivo electrónico embebido inalámbrico (hardware) de bajo consumo energético desarrollado desde cero, y energía solar fotovoltaica. El dispositivo embebido incluye firmware especializado y un protocolo de comunicación inalámbrico energéticamente eficiente, que permite conformar una red de sensores infrarrojos de detección de peatones y vehículos, para el control y regulación de intensidad de las luminarias LED. Un piloto fue instalado en una calle aledaña al campus de la Universidad Privada Boliviana en la ciudad de Cochabamba, Bolivia, donde se realizaron medidas del consumo energético del sistema, que confirman un ahorro energético del 72.8% gracias al control inteligente desarrollado.

Palabras Clave: Sistema de Iluminación Vial, Sistema Fotovoltaico, Sistema de Control Inteligente Inalámbrico, Eficiencia Energética.

1. INTRODUCTION

Street lighting is essential for citizen and road safety. It can be used to increase urban security by improving safety for drivers, riders, and pedestrians. Driving at night is more dangerous than driving in any other moment of the day - only a quarter of all travels by car drivers are made during the nighttime (between 7pm and 8am), yet this period accounts for 40% of fatal and serious injuries. In this context, also pedestrians and vulnerable road users suffer from decreased visibility in the dark [1]. The studies in [2, 3] suggest that street lighting deployment may prevent road accidents and fatalities and significantly reduce crime. In this sense, another study [4] suggests that, when risk for citizens are considered carefully, techniques for power consumption reduction in street lighting (i.e. light dimming, light switch off) can be applied without affecting pedestrian security.

Street lighting currently has two major flaws and drawbacks. On the one hand, it represents an energy consumption problem, accounting for 19% of the global use of energy and approximately 6% of greenhouse gas emissions [5]. This is mainly due to the inefficiency of conventional street lighting systems, as they operate continuously throughout the night, regardless of the presence of pedestrians or vehicles. On the other hand, in Bolivia and other developing countries, street lighting systems in some peripheral areas are either deficient or nonexistent, due to the fact that electricity transmission and distribution systems do not cover the entire territory [6].

Reducing CO₂ emissions and achieving energy efficiency is a core factor for the transition towards a resource-efficient economy and the smart sustainable growth the world is seeking today. Street lighting is an important part to achieve this goal, where the highest amount of energy consumption related to it, is caused by inefficient legacy systems. Strong financial and technological drivers suggest that billions of dollars around the globe could be saved in energy costs per year by switching to light-emitting diode (LED) technology. LED lights provide two major benefits: reduce power consumption and have longer service life, which is three to five times longer than legacy lighting technologies [7]. This increase in service lifetime is also reflected in an important reduction of costs for maintenance. Moreover, this technology is far more flexible than legacy systems, by enabling the application of smart or intelligent electronic control to adjust LED dimming to reduce energy consumption [5].

Therefore, traditional street lighting systems must be re-designed with an energy-efficiency scope on all the systems involved. Firstly, loads must be optimized, replacing High Pressure Sodium (HPS) lamps, or similar technologies, with LED. In this way, an efficient conversion of electric energy into light is ensured. Secondly, using optimized loads, it makes sense to replace the source of electrical energy with renewable and clean energy, such as photovoltaic (PV) solar energy. The use of PV systems avoids using fossil resources, thus minimizing the impact on greenhouse emissions. In addition, thanks to their great portability, simple installation, long-service life and the high availability of the solar resource, makes PV systems an effective option for isolated electrification systems for street lighting in developing countries with good solar radiation conditions [8], as is the case for Bolivia [9]. Thirdly, reducing the energy waste from having the street lighting at 100% of its power all the time, to an adaptive solution that varies the light intensity according to vehicles and pedestrian traffic, to achieve energy savings.

In this paper, we describe a new smart street lighting system based on renewable energy, that follows the aforementioned aims. The contributions of this paper include:

- the design, pilot implementation and testing of an energy-efficient street lighting system (Smart Renewable Energy Street Lighting - SRESLi), which allows to intelligently adapt light intensities according to the traffic of pedestrians and vehicles;
- the design and implementation of specialized hardware, an embedded control device - the SRESLi System Unit - which features a proprietary energy-efficient wireless communication protocol;
- the optimization of energy consumption through a PV solar system for providing electric power to the SRESLi System Units and LED lamps to obtain expected lighting conditions; and
- achieving energy efficiency while taking care of citizen and road safety, thus finding the adequate balance between energy consumption reduction (i.e. light dimming) and pedestrian security to guarantee road safety.

The rest of this article is structured as follows: Section 2 states the related work. Section 3 describes the complete design and development of the SRESLi and the PV system. Section 4 includes the experimental setup, deployment of the pilot system, and measurements of lighting levels and power consumption with and without SRESLi. Section 5 concludes the article.

2. RELATED WORK

In current smart street lighting systems, we can distinguish six key components: Communications, sensors, processing power, dimming system, system-fault monitoring and power consumption. In terms of communications for smart light control, two main approaches exist: wired communications with Power Line Communications (PLC) and wireless sensor networks (WSN) like the ZigBee stack [5, 10]. In general, the preferred choice is WSN, due to major drawbacks from wired technologies regarding heavy deployment, installation costs and maintenance. Furthermore, the wireless alternative offers low-cost, easy installation, and scalability [5]. Another type of wireless communications technology, GSM, is often used in centralized street lighting systems mainly to report failures [11-13].

Regarding light dimming systems, three common techniques stand out for street lighting: The first one consists of an optimized on/off switch driven by the detection of an object of interest, e.g., using image processing [11]. The second approach consists in dimming on demand through Pulse Width Modulation (PWM) brightness control [13]. Finally, the last approach introduces the next level of 'intelligence' by implementing adaptive traffic control based on probability models acquired by observation of traffic volume on a specific road [5]. All the aforementioned approaches use solar energy with PV systems independent from the conventional electric grid. In [14], a street lighting system is proposed, by combining both PV and grid energy systems, achieving positive yearly energy balance an intelligent control system thanks to the use of infrared motion sensors measuring the speed and the direction of the motion in the proximity of the luminaire. Smart controllers, in turn, classify these motion signals as vehicle traffic, pedestrian traffic, or no traffic, and adjust their dimming levels to the detected scenario.

Existing approaches for intelligent control systems, are based on off-the-shelf electronics for signal processing (e.g., RaspberryPi, Arduino, ATmega16, AT89S52), sensor hardware and communication modules (e.g., Zigbee, GSM, Wifi,

Bluetooth). Even though some of the processing units and communication modules are designed for low-power consumption, they may require the development of customized protocols to avoid, e.g., constant signal sensing, which prevents optimizing the power consumption of the electronic control system itself. This is for example, the case of Zigbee technology, for which current communication protocols support beacon and non-beacon enabled networks. In non-beacon-enabled networks, an unslotted CSMA/CA¹ channel access mechanism is used, having their receivers continuously active, and therefore requiring more power supply. In beacon-enabled network, normally sleeping network slave nodes wake up periodically to receive a synchronizing "beacon" from the network's control node. But listening for a beacon wastes power too, particularly because timing uncertainties force nodes to turn on early to avoid missing a beacon. One alternative is therefore to use TDMA²-based protocol (based on IEEE 802.15.4 on the MAC layer of Zigbee) and design an energy-efficient custom hardware for both processing and communication. This is the approach followed for SRESLi for energy efficiency.

3. DESIGN AND IMPLEMENTATION OF SRESLI

The SRESLi system prioritizes and controls light dimming according to pedestrian and vehicle traffic, thus, controlling energy consumption and promoting energy savings when compared with traditional street lighting. The system was designed to achieve maximum energy efficiency through a combination of wireless embedded electronic control, LED technology and photovoltaic energy.

The proposed system can detect road users (i.e., pedestrians or vehicles) inside the operating environment and adjust the streetlight illumination according to their flow. When some user is detected within the operating environment, the illumination decision is communicated to neighbor SRESLi-enabled light-poles near to the identified users. Additionally, the SRESLi System Units can enter different operation modes to save energy and be functional only when is needed. Figure 1 shows the system environment and actors.

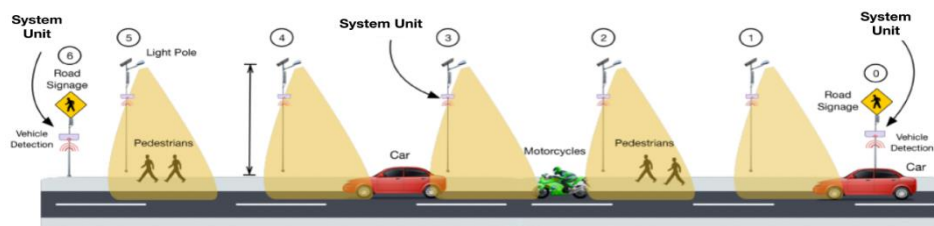


Figure 1: SRESLi system environment and actors.

The SRESLi system can be divided into three subsystems: the wireless embedded electronic control system, the LED street lighting system, and the photovoltaic system, that are described in the following subsections.

3.1 WIRELESS EMBEDDED ELECTRONIC CONTROL - THE SRESLI SYSTEM UNIT

The wireless embedded electronic control subsystem of SRESLi (called in the following the "SRESLi System Unit"), is a custom hardware device that we designed and developed from scratch for energy efficient street-lighting control. The SRESLi System Unit also features a proprietary communication protocol and a firmware to reduce the power consumption and to avoid a centralized decision system.

Hardware Design

The hardware design of the SRESLi System Unit includes the unit hardware interface, the unit hardware blocks and the printed circuit board (PCB) that are described in the following:

- *Unit Hardware Interfaces*

Every SRESLi System Unit is composed of three main hardware interfaces that allow communicating with other units:

- **Radio Interface:** This hardware interface is the 2.4GHz radio which is compliant with IEEE 802.15.4 specification [15]. This interface represents the physical layer of our developed communication protocol.

¹ Carrier-Sense Multiple Access with Collision Avoidance (CSMA/CA)

² Time Division Multiple Access (TDMA)

- **Light Dimmer Interface:** allows the SRESLi System Units to communicate with the LED light dimmer (located in the same light pole) to send commands for turning on or off the LED light and control the light intensity. This interface uses a serial communication with RS-485 standard [16, 17].
- **Expansion Interface:** allows to extend the hardware functionality of the SRESLi System Unit. This interface is able to be configured programmatically to communicate to the additional hardware expansion modules or to provide enhanced functionality, e.g., connecting additional sensors, actuators, other types of communication modules.

Figure 2 shows the SRESLi System Unit hardware interfaces that communicate with other functional units of the system, either locally or remotely.

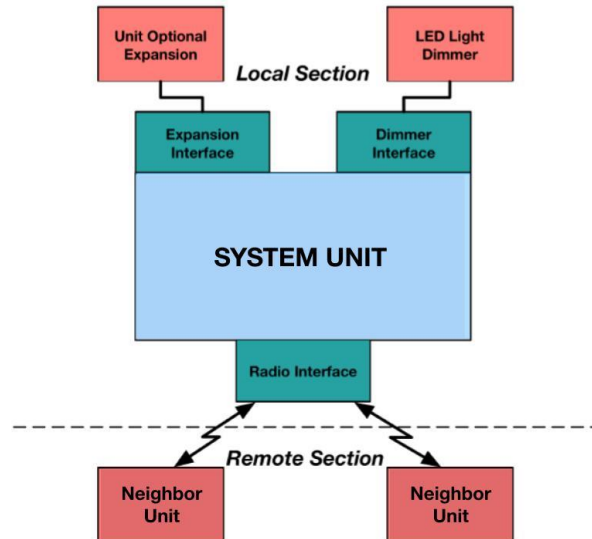


Figure 2: The SRESLi System Unit hardware interfaces.

▪ Unit Hardware Blocks

To satisfy the technical specifications, 5 blocks were defined in the hardware design:

- **Wireless Microcontroller:** Main processing unit of the device that includes a 2.4GHz radio transceiver compliant with the IEEE 802.15.4 specification.
- **Current sensor:** Measures the current flow and its direction. This block is used to measure the power supply provided by the solar panels during the day (current flow from the solar panel to the energy storage and the system), or by the energy storage during the night.
- **PIR array sensor:** Passive Infrared (PIR) sensor that detects the presence of pedestrians and vehicles inside the system boundary.
- **RS-485 Transceiver:** Allows the communication of the systems units to their corresponding LED dimmer to control the light intensity of the luminaire.
- **DC-DC Regulator Power supply:** Provides a fixed operating voltage for the unit by regulating the voltage input.
- **RGB LED:** Used for debugging purposes and feedback signaling.

Figure 3 shows the hardware block diagram of the SRESLi System Unit and the corresponding hardware interfaces.

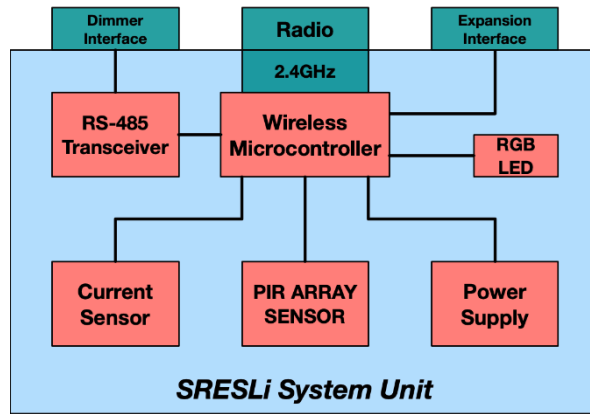


Figure 3: SRESLi hardware block diagram.

▪ SRESLi System Unit PCB

The SRESLi System Unit consists of a two-layer PCB design for RF communication (2.4GHz). Figure 4 shows the SRESLi System Unit PCB with all the hardware blocks and interfaces mounted on the PCB board. All hardware components, connectors and most traces are located in the top layer. SRESLi System Unit PCB design followed all the recommendations from the microcontroller manufacturer described in [18]. However, the prototype design was implemented into a two-layer PCB in order to reduce manufacturing costs. Even though RF design recommendations suggest working on four layers PCBs, SRESLi System Unit’s performance was not affected during hardware validation tests for communication. Figure 4 shows the SRESLi System Unit finished prototype after PCB manufacturing and electronic component assembly processes. In addition, Figure 4 presents the locations and descriptions of the most important components, connectors, and interfaces.

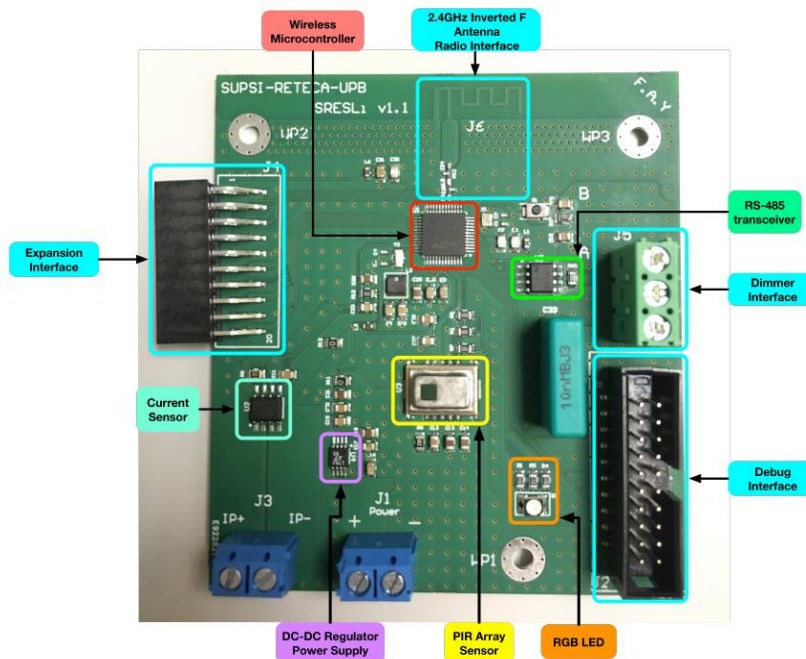


Figure 4: The SRESLi System Unit PCB Description.

Communication Protocol

As mentioned before, a smart street lighting system requires communication between its units to control the light intensity of LED lamps. For this reason, we developed a communication protocol allowing the transmission and reception of light control commands. In addition to the light control application, the protocol provides an energy efficient access to the medium by using a TDMA approach. Figure 5 shows the network layers where the protocol was developed. Also, is possible to see that IEEE 802.15.4 specification is defined at Physical and Data-Link Layers. For this purpose, the wireless microcontroller provides all the specification functionality in its integrated transceiver. In this way, the chosen wireless microcontroller uses the following default configuration for the specification: O-QPSK³

³ Offset Quadrature Phase-Shift Keying (O-QPSK)

modulation at 2.4 GHz at the Physical layer and CSMA/CA channel access mechanism at Data-Link layer. In our communication protocol, we changed the way of accessing the channel to TDMA. In this way, energy efficiency is improved by solving the need to continuously sense the communication channel by the CSMA/CA approach. In consequence, the SRESLi protocol is mainly built upon the physical layer of IEEE 802.15.4 specification.

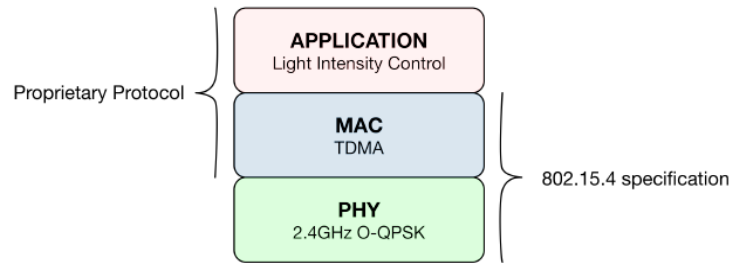


Figure 5: Network layers of SRESLi communication protocol.

▪ *Communication Architecture*

One of the major challenges in TDMA communication approach is the timing control, because each node in a Wireless Sensor Network (WSN) has an inaccurate hardware clock reference (crystal oscillator). In the case of TDMA, clock offset and clock drift from each network node has to be compensated in order to have a precise common timescale over the network.

Figure 6 shows the communication architecture of the SRESLi network. In the figure, is possible to distinguish five SRESLi System Units deployed in each light pole along a street. The network follows a simple tree topology and according to the physical position on the street, every unit has a specific address (physical address) and a specific role in the network. The role of each node in the network is fundamental at synchronization phase for the TDMA approach that governs the medium access. Three types of nodes are presented according to their functionality during the synchronization phase:

- **Level 0 - Root Node:** Unique type of node in the network, is the most important since provides the clock reference for the other communication nodes . There is only one root node in the entire network that provides a clock reference for the other nodes.
- **Level 1 - Mid Nodes:** This type of node is located between the root node and the end nodes. Mid nodes receive a clock reference from their parent (root node) and also provide a clock reference for their potential children (end nodes).
- **Level 2 - End Nodes:** Located physically at the edges (beginning or end) of the street that is being covered. This type of node only receives a clock reference from their parents (mid nodes).

Once the network nodes are synchronized, the data transmission begins. The data transmitted and received between the nodes carry the events occurred at each light pole. Later, the light control application from each SRESLi System Unit process and identifies events in the received data in order to control the LED light dimmer.

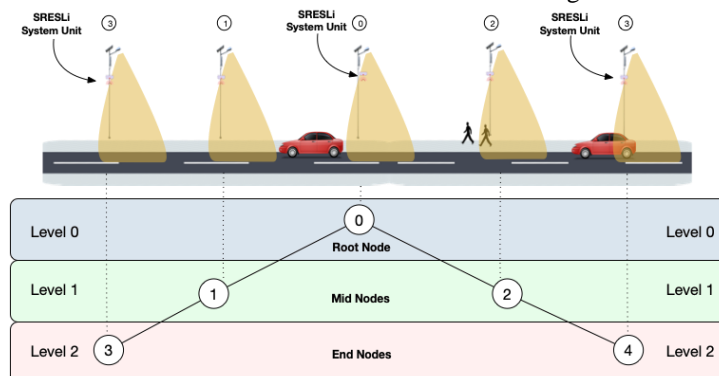


Figure 6: SRESLi Communication Architecture.

▪ **Protocol Packet Structure**

SRESLi communication protocol consists of two major stages in TDMA mode: Synchronization and Data transmission. Each stage demands a specific data packet; those packets are described in Figure 7.

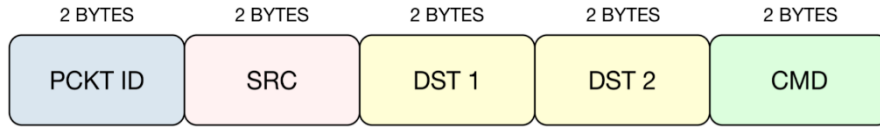


Figure 7: SRESLi Protocol: Synchronization Packet Structure.

- **Synchronization Packet:** Synchronization packet has a fixed length of 10 Bytes, composed by five fields: Packet ID (PCKT ID), Source, (SRC), Destination 1 (DST 1), Destination 2 (DST 2) and Command (CMD). Each field has a size of 2 Bytes. Figure 7 shows the packet structure of the Synchronization Packet and Table 1 describes each field and its values.
- **Data Packet:** As in the previous case, Data packet has a fixed length of 10 Bytes, composed by five fields: Packet ID (PCKT ID), Source, (SRC), Destination 1 (DST 1), Destination 2 (DST 2) and Event (EVENT). Each field has a size of 2 Bytes. Figure 8 shows the packet structure of the Data Packet. and Table 2 describes each field and its values. The application layer field includes the three types of events that need to be sent to the neighbor nodes for light control when pedestrians, vehicles or both are detected.

TABLE 1 - SRESLI PROTOCOL: SYNCHRONIZATION PACKET FIELD VALUES

Field	Description
PCKT ID	Packet Identifier: - 0x000A: Synchronization Packet
SRC	Node Source Address: - 2 Byte Network address value
DST 1	Destination Address 1: - 2 Byte Network address value
DST 2	Destination Address 2: - 2 Byte Network address value
CMD	Synchronization Command: - 0x00A0: Sync. Command Initialization - 0x00B0: Sync. Response - 0x00C0: Sync. Ready

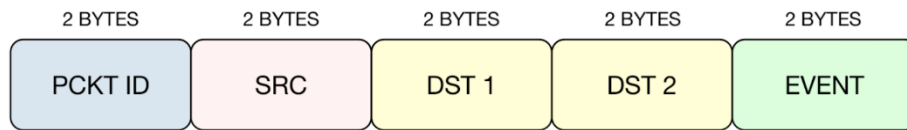


Figure 8: SRESLi Protocol: Data Packet Structure.

TABLE 2 - SRESLI PROTOCOL: DATA PACKET FIELD VALUES

Field	Description
PCKT ID	Packet Identifier: - 0x000B: Synchronization Packet
SRC	Node Source Address: - 2 Byte Network address value
DST 1	Destination Address 1: - 2 Byte Network address value
DST 2	Destination Address 2: - 2 Byte Network address value
EVENT	Event Detected by the system, corresponds to

(Application Layer)

Protocol Application Layer:

- **0x00F0**: Pedestrian Detected
- **0x000F**: Vehicle Detected
- **0x00FF**: Pedestrian and Vehicle Detected

▪ *MAC Layer: TDMA Channel Access Approach*

- **Synchronization:** Time synchronization follows a simple flood mechanism, starts at the root node in level 0, continues through level 1 with the mid nodes and then finishes in level three with the end nodes. If the sequence fails at any level, the procedure is started again in the next synchronization period by waiting again for a synchronization command (Sync. CMD) from the parent node at a higher level.
- **Data Transmission and Reception:** Data transmission and reception starts after successful node synchronization. Each node has specific transmission and reception time window intervals.

Firmware Design

Embedded firmware stores specialized software running in embedded device to control its functions and also to interconnect with additional equipment. SRESLi system units include firmware to execute the main application and to control light intensity.

▪ *Main Firmware Application*

The main firmware is composed of four tasks: Hardware configuration, sensor data acquisition (data acquisition from current sensor and PIR array sensor), sensor data processing and communication. Figure 9 shows the main application tasks in a flowchart.

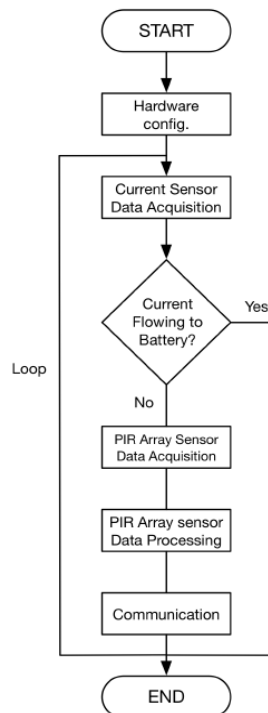


Figure 9: SRESLi's firmware application flowchart.

The last three tasks have periodic execution intervals and together form the main loop of the program. In order to have a better time control for each task, we implemented from scratch a Round-Robin scheduling scheme, ensuring that the execution intervals are respected. When the SRESLi System Unit is running in sleep-mode (i.e., during the day when there is enough sunlight and current flows to the battery), the execution of data processing and communication tasks are skipped. The program waits until the entire loop duration finishes before starting with the tasks again, i.e., the task interval is always respected, and a fixed sample rate is achieved. Figure 10 shows the task execution scheme, where the main loop duration is of 150 ms, and each of the three tasks (PIR sensor data acquisition, data processing and communication) are divided in slices of 50 ms.

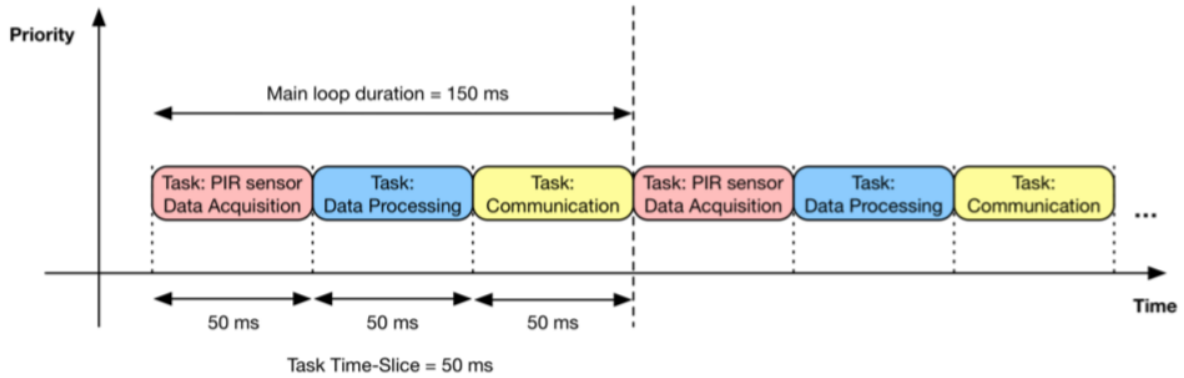


Figure 10: Task execution using Round-Robin scheduling scheme.

▪ **Light Intensity Control Application**

The light intensity control application follows 3 different use-cases: pedestrian, vehicle, and simultaneous pedestrian and vehicle. To control the light, the collected local and neighbor events are analyzed. The behavior of the light intensity control is described in the state-machine shown in Figure 11. The state machine has three states representing the percentage of light intensity (i.e., 10%, 50% and 100%). After the initial state, the lights are turned-on to the default 10% of intensity. When an event is detected by the sensor or communication unit (i.e., a command from a neighbor), it is analyzed to identify the aforementioned use-cases. In the case of a vehicle, the light intensity is increased to 50% and a command signal is sent to the neighbor (depending on the direction of the vehicle). Similarly, if pedestrians are detected, the light intensity is increased to 100%. If pedestrians and vehicles are detected simultaneously, the control gives priority to pedestrians. In all cases, a timeout is set and on expiration, the intensity is reduced to the default one if no other event arrives. This control scheme ensures that the energy consumption is dynamically adapted to the traffic, thus saving energy when no event happens.

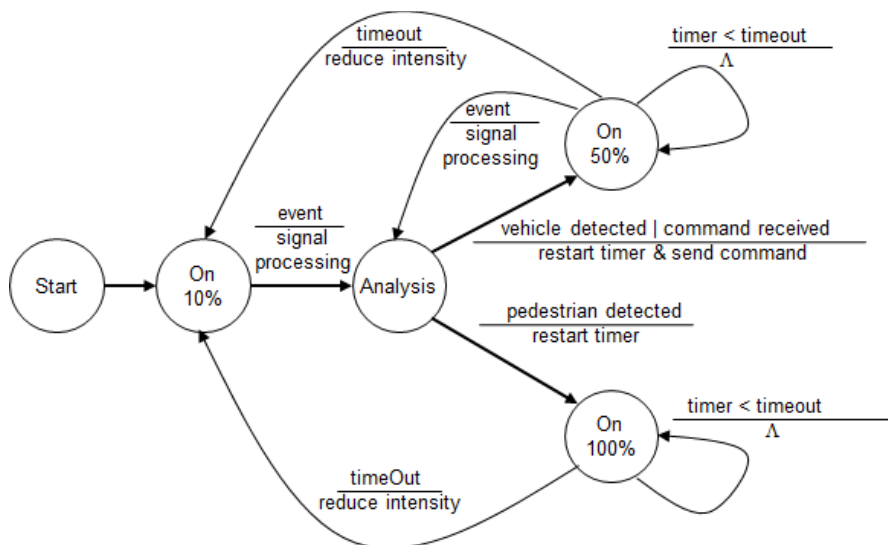


Figure 11: Light intensity control state-machine.

Energy consumption

The DC-DC power supply of the SRESLi System Unit provides and measures a fixed stable voltage for all the electronic components and peripherals inside the device. The operation voltage of all electronics components is 3.3 V, hence a DC-DC regulator was chosen to take an input voltage from a higher range and provide a fixed output voltage of 3.3 V.

We calculated the current required by the SRESLi System Unit for the full operation mode (i.e., with PIR sensor data acquisition, data processing and communication), since this mode is where the systems consumes current the most. Table 3 shows the current consumption of the components used in the SRESLi board. We selected a EFR32FG Radio 2.4GHz and microcontroller [19], a Grid-Eye PIR Array sensor from Panasonic [20] and ACS711 Current sensor, a SP3485 RS-485 Transceiver for serial communication [21] and a LED. The chosen regulator, LT1762 from Linear

Technologies [22], was selected considering the current required by the board and the output current provided by the integrated circuit and the input voltage range. The LT1762 is a low-noise low-dropout DC regulator that provides an output current of 150 mA and supports an input voltage range between 1.8 V and 20 V. The total average current required for the SRESLi System Unit in full operation mode is of 80 mA, which represents at 3.3 V, a power consumption of 0.26 W. This confirms that our hardware design is highly energy efficient.

TABLE 3 - CURRENT CONSUMPTION OF THE SRESLI SYSTEM UNIT IN FULL OPERATION MODE

Component	Current [mA]
EFR32FG Radio 2.4GHz @ max power	42
Microcontroller EFR32FG	3
PIR Array sensor - Grid-Eye	5
Current sensor - ACS711	6
Transceiver RS-485 SP3485	4
RGB LED (one LED)	20
Total current consumption	80

3.2 LED street lighting

The LED street lighting subsystem of SRESLi has the following requirements:

- have the lowest possible power consumption while providing the required lighting;
- have the ability to regulate light dimming in order to be controlled by the SRESLi System Unit; and
- comply with the lighting levels imposed by the Bolivian regulation for street lighting NB 1412001 [23]

Based on these requirements, we selected lamps of type Sword LED Street Light - LEYOND of 50W of power, which have the best tradeoff between power, availability in the market and cost. Then, we used the Relux lighting design software [24] to determine important deployment parameters such as the distance between luminaires and the installation height where the LED need to be placed. We categorized the road according to its flow, type, width, and lighting category according to the public lighting standard. We then run the simulation in Relux, determining the height and spacing, the geographical location of the poles for the experimental setup of the system.

3.3 Photovoltaic system

The photovoltaic subsystem of SRESLi includes the daily electrical consumption and the photovoltaic field parameters, so as to select the most adapted components and the sizing of the PV system.

Electrical Consumption

To determine the daily electrical consumption of the system it is important to establish the complete load of power consumption, the operating period, and the consumption factor. As a load, we considered both the lamp (with a 55W power consumption), the SRESLi System Unit (with a 0.26 W power consumption) and the dimmer interface (with a 0.2 W power consumption). The operating time of the system is of 12 hours, which represents the average daily value (calculated over one year of the operation) of a conventional public lighting [7, 25]. In addition, it is important to consider the consumption factor, which corresponds to the percentage of time that the load will work at maximum electrical power, so as not to oversize the system.

Table 4 shows the daily electrical consumption of each LED lamp, the Dimmer Interface (based on an Arduino UNO device), and the SRESLi System Unit, with a total consumption of 665.52 Wh/day. Based on this result, the sizing of each solar panel gives a peak power (P_{peak}) of 189.93 Wp according to equations (1) and (2) [35], where, E is the daily energy consumption (i.e., 665.52 Wh/day); $\eta_{general}$ is the performance ratio or general performance (i.e., 80% according to [26] which considers a 0.95 PV efficiency, 0.9 battery efficiency, 0.98 wiring efficiency and 0.95 inverter efficiency); T_{min} is the minimal amount of hours per day with solar radiation (i.e., 4.38 Solar Peak Hours calculated according to [27] with data from the NREL-NASA for the location coordinates).

$$E_{required} = \frac{E}{\eta_{general}} \quad (1)$$

$$P_{peak} = \frac{E_{required}}{T_{min}} \tag{2}$$

However, since we know that our system will save energy, using the obtained peak power of 189.93 Wp, represents a highly oversized value and a high cost. In addition, we would need to measure the energy saving for an accurate sizing of the required PV system, which is not possible until the complete installation and measure of the real power consumption of the system. Fortunately, we can mitigate the oversizing issue, by taking as reference existing similar intelligent street lighting systems [5,10,13], which achieve savings between 68% and 82%. We therefore consider a conservative energy saving of 50% for the sizing of our PV system, resulting in a final peak power of 94.9 Wp for the component sizing and selection.

TABLE 4 - DAILY ELECTRICAL CONSUMPTION OF EACH LUMINAIRE

Load Type	Power [W]	Daily Electrical Consumption [Wh/day]
LED Lamp	55	660.00
Dimmer interface (Arduino UNO)	0.2	2.40
SRESLi System Unit	0.26	3.12
	TOTAL	665.52

Components Sizing and Selection

The pilot system is located at the main campus of the Universidad Privada Boliviana (UPB) in the city of Cochabamba, Bolivia (at coordinates latitude = -17.399126° and longitude = -66.2178536°). Because the orientation of solar panels would affect solar radiation parameters for the calculation, we considered the city location in the southern hemisphere of the globe to calculate the photovoltaic field [27], resulting in an inclination of 22.17° and an Azimuth of 0°. The average value of solar intensity in the pilot coordinates is about 600 W/m2 [9].

TABLE 5 - SELECTED COMPONENTS OF THE PV SYSTEM

Units	Components	Size [Unit]	Type
1	PV panel	100 [Wp]	LORENTZ LC100-M36 [28]
1	Controller	8 [A]	PHOCOS CML 8 [29]
1	Battery (PB-Acid)	70 [Ah]	TOYO SOLAR 70Ah [30]
1	Inverter	375 [VA]	PHOENIX INVERTER 375 VA [31]

Based on the previously calculated daily electrical consumption, the photovoltaic field characteristics, and the local solar intensity, we calculated the components sizing using the conventional sizing method [35], which is shown in Table 5, for each pole.

System Design

Once the sizing of the PV system components was set, we include the integration with the SRESLi System Unit and a connection to the conventional 220V electric grid (for backup energy). Figure 12 shows the deployment diagram for each light pole of the system.

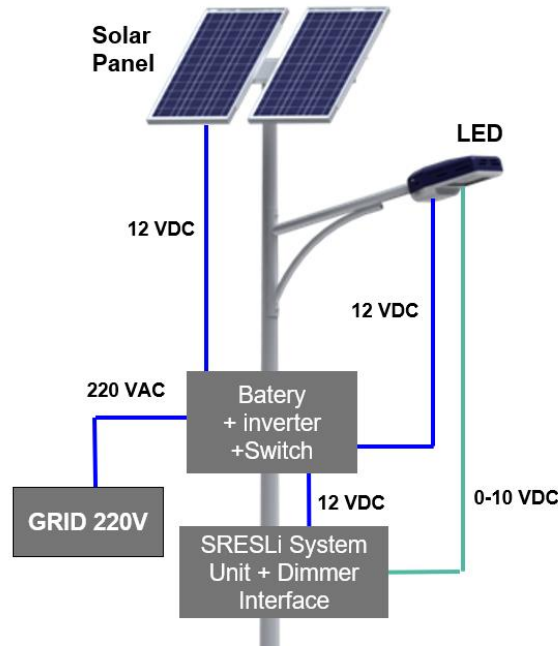


Figure 12: Deployment diagram for each light pole.

Following the proposed deployment and integration scheme, we designed the final system architecture (see Figure 13), where the voltage levels of each connection are shown (whether it is of 12 V, 220 V or electronic control). The figure shows a switch that allows to select the energy source which can be autonomous (i.e., from the PV system) or the conventional electric grid. The switch is operated manually, and the system uses the conventional electric grid, in the case of climate conditions, not allowing to have enough solar intensity. The PV system, stores energy in the battery, which requires a charger controller that handles the current entering the battery, as well as the energy that is used by the electrical loads (i.e, the LED lamp, the SRESLi System Unit, and the Dimmer Interface). Because the voltage that uses the LED luminaire is of 220 VAC, and the battery provides 12 VDC, we use a DC-AC inverter connected to the battery through the charge controller. Furthermore, to dim the LED luminaire intensity, a Pulse-Width Modulation (PWM) is required in a 0 to 10 V interval, which corresponds to a 0 to 100% light intensity. The SRESLi System Unit sends a digital control signal through a RS485 serial communication, that needs to be converted to a PWM, which is done by the Dimmer Interface based on an Arduino UNO and an additional electronic circuit using a NPN BC639 [32] (not shown in the figure). Finally, depending on the event detected by the sensor, the decision is sent to the neighbor SRESLi System Units, using the previously described communication protocol through the 2.4 GHz Radio.

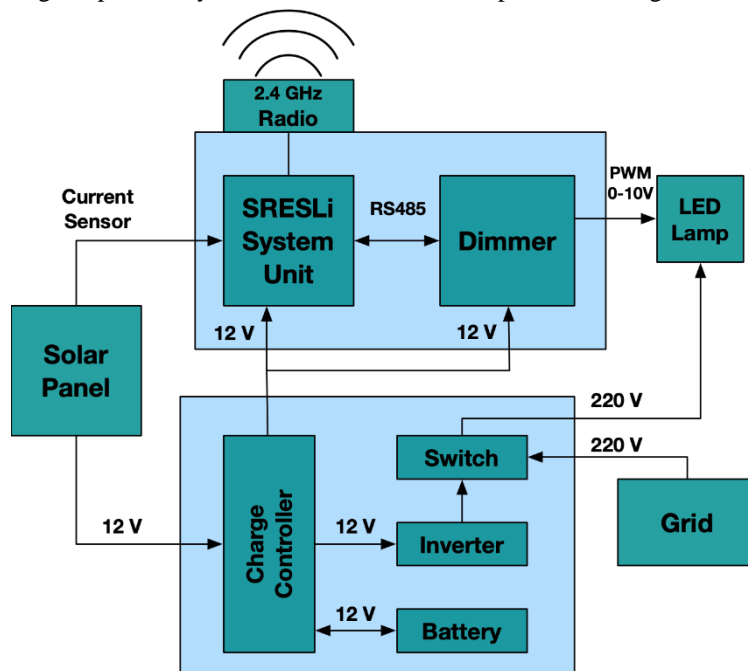


Figure 13: Complete system's architecture diagram

4. EXPERIMENTAL SETUP AND RESULTS

A SRESLi pilot was implemented at Universidad Privada Boliviana as the experimental setup to measure lighting levels, energy generation and power consumption. The pilot includes five light poles deployed on the campus back road, a poorly illuminated road with medium to low vehicular and pedestrian traffic. The light poles had a 15m distance between each other and the lamps were fixed at a height of 7m. Figure 14 shows the poles distribution and Figure 15 shows the implementation of one light pole.



Figure 14: Pilot system deployment scheme.



Figure 15: Implemented light pole.

Figure 16 shows the complete pilot system running at its maximum intensity during the night. The figure shows a comparison between our LED-based pilot (on the left) w.r.t. the existing street lighting based on High Pressure Sodium - HPS (on the right). We can see a clear improvement in the visibility and a homogeneity of lighting in the left-side part of the figure. Also, the LED-based street lighting eliminates the monochromatic black appearance of object illuminated by the HPS, thus providing a much better variety of high Color Rendering Index (CRI)⁴.



Figure 16: The complete deployed pilot system, comparing LED luminaires and High-Pressure Sodium luminaires.

4.1 Lighting levels

In order to measure the lighting distribution between the poles, we measured the illuminance in lux at each point of a measuring matrix using a luxometer⁵ attached to a tripod, so as to hold the sensor perfectly parallel to the ground as shown in Figure 17. Figure 18 shows the matrix with 15 points of measurements. It divides the 15 meters of distance between the poles (S) into 5 segments and divides the street width (A) into three segments (B, C, and D). Figures 19, 20 and 21 show the spatial distribution for a 10%, 50% and 100% lighting level, respectively. We can observe in these spatial distributions, that the illuminance at the ground level between the poles, do not create gaps. This confirms the homogeneous LED-based lighting, shown in the left-side of Figure 16.

⁴ <http://www.cie.co.at/publications/colour-rendering-white-led-light-sources>

⁵ We used an EXTECH Instruments (Fc/lux) - model 401025 (http://www.extech.com/resources/401025_UM.pdf)



Figure 17: Luxometer on tripod.

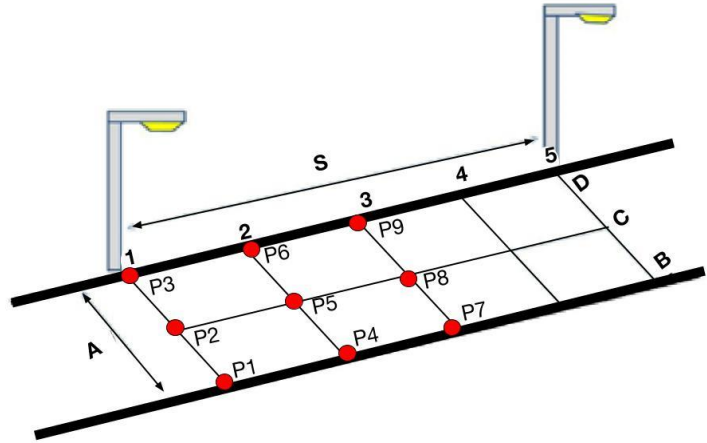


Figure 18: Illuminance measurements matrix.

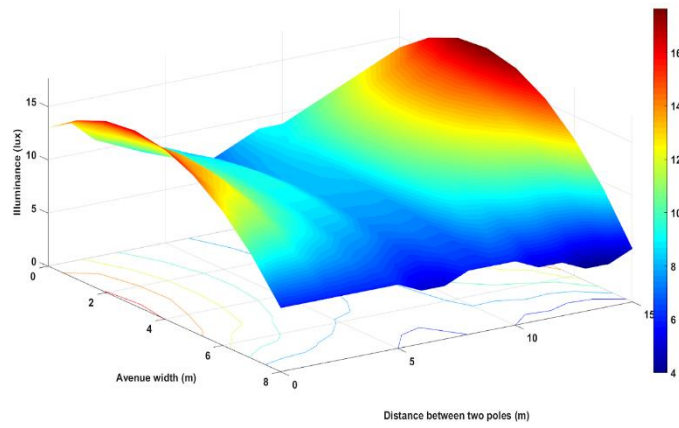


Figure 19: Spatial distribution of illuminance of the system at 10% lighting level

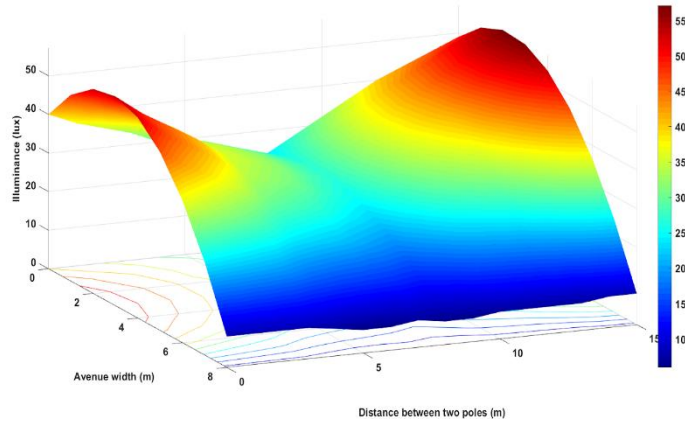


Figure 20: Spatial distribution of illuminance of the system at 50% lighting level.

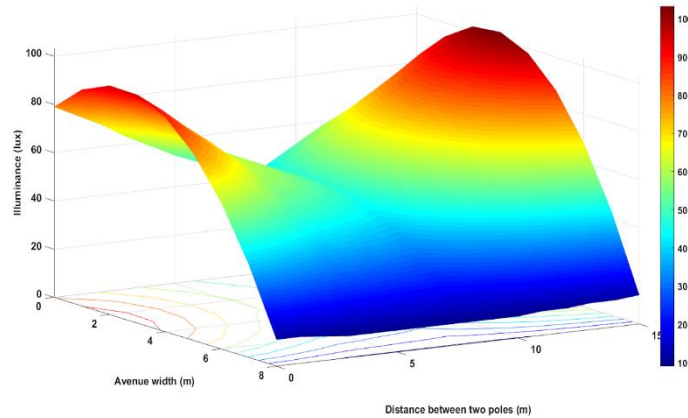


Figure 21: Spatial distribution of illuminance of the system at 100% lighting level.

In order to determine whether the illuminance of our pilot complies with Bolivian regulations for street lighting [23], we measured the average illuminance applying the nine-points method [33,34] in the measurement matrix. We calculated the average illuminance in the three lighting levels (10%, 50% and 100%) in which the system operates. The measurements were made between light poles that are not those in the border.

Table 6 shows the results obtained with the nine-point method, where E_i is the illuminance of each measured point ($i = 1 \dots 9$), E_{avg} is the average illuminance, and E_{min} and E_{max} are the minimum and maximum illuminance, respectively. The average illuminance calculated for each lighting level is as follows: 9.8 lux for a 10% lighting level, 29.7 lux for a 50% lighting level, and 51.9 lux for a 100% lighting level. These results confirm that, even at the lowest level of intensity, the system operates according to the Bolivian regulations for street lighting, which requires an average illuminance between 5 and 10 lux [23].

TABLE 6 - RESULTS OBTAINED WITH THE NINE-POINTS METHOD

		Illuminance [lux]											
		E_1	E_2	E_3	E_4	E_5	E_6	E_7	E_8	E_9	E_{avg}	E_{min}	E_{max}
Lighting Level	10%	5.5	16.0	14.0	5.5	11.0	10.0	6.0	8.0	8.0	9.8	5.5	16.0
	50%	8.0	55.0	46.0	7.0	36.5	35.0	7.0	25.0	24.0	29.7	7.0	55.0
	100%	12.0	96.5	82.5	9.5	66.0	60.5	9.0	45.0	40.0	51.9	9.0	96.5

4.2 Power generation, consumption and intelligent control

Once the pilot was deployed and the spatial distribution of illuminance were measured, we proceed to measure the power generation of the PV system, the consumption of the luminaires to validate the energy efficiency thanks to the intelligent control of the SRESLi System Unit.

a. Power Generation

To determine whether the PV system generates enough electricity to work properly (for both the lighting and electronic control system), we collected power generation measurements using two data logging multimeters⁶. One multimeter was used to take current measures and the other to take voltage measures as shown in Figure 22. Under this scheme, we used a 5 minutes measurement interval throughout the entire day in each of the 5 poles.

⁶ We used Fluke 289 True-RMS Data Logging Multimeters (<https://www.fluke.com/en/product/electrical-testing/digital-multimeters/fluke-289>)

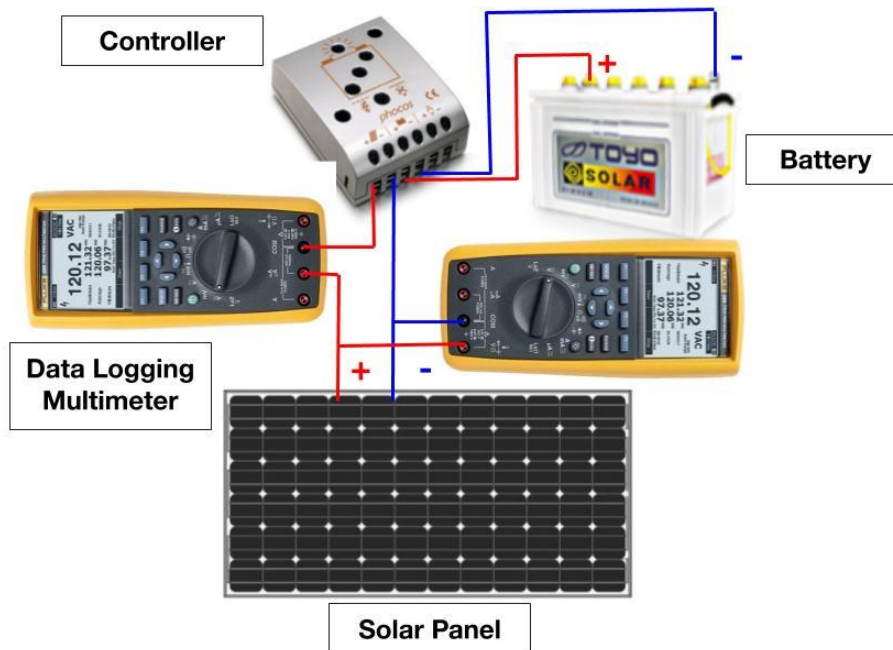


Figure 22: Power generation measurement scheme.

Figure 23 (left) shows the average power generation for one PV panel in each pole throughout a day (12 hours). The average generated energy is represented by the area under the curve, and is 457.1 Wh. Figure 23 (right) shows the measured current flow to the battery, allowing to determine a stored energy of 359.8 Wh. The amount of generated energy is clearly not enough to power all the loads of the luminaire (i.e., LED lamp, SRESLi System Unit, and Dimmer Interface) for 12 hours operation time, which requires 665.52 Wh/day (see Table 4). We therefore proceed to measure the actual power consumption in two scenarios:

- without the SRESLi System Unit: to determine the maximum amount of time that the stored energy allows to power one street lighting luminaire at its full intensity; and
- with the SRESLi System Unit: to show the intelligent adaptive lighting with energy efficiency, and that the stored energy is enough to operate more than 12 hours.

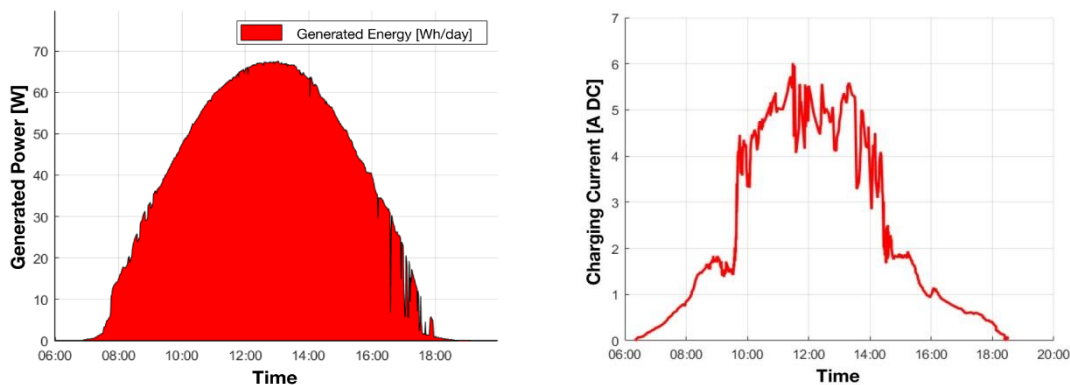


Figure 23: Average generated power (left) and the charging current circulating to a battery (right), throughout a day of one PV panel.

b. Power consumption without the SRESLi System Unit

We measure the power consumption of the system without the SRESLi in one street lighting luminaire at 100% of its capacity over a full night. A data logging multimeter is used to measure the AC current consumption using a default 5-minute intervals, but also registering any sudden current change in between the intervals to identify all patterns of consumption changes. Figure 24 shows the total consumed power which drained the battery in 6.5 hours, covering only half of the required energy (at 100%). Thus, through this experimental measurement, we obtain that the total consumption in 12 hours is about 665 W, which is closed to the previously estimated value of 665.52 Wh/day of 12 hours (see Table 4).

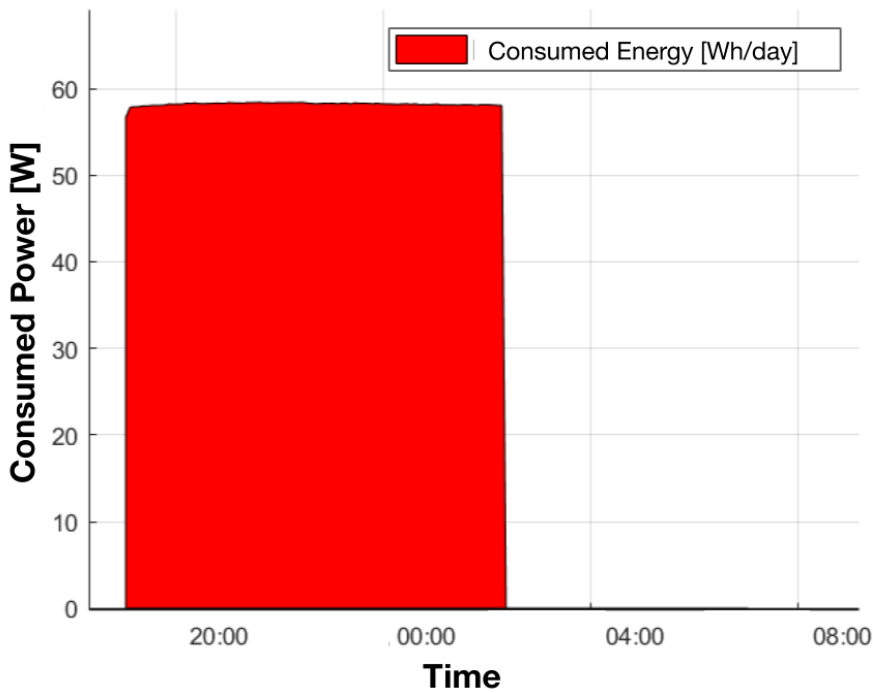


Figure 24: Power consumption for one luminaire throughout the night without the SRESLi System Unit.

c. Power consumption with the SRESLi System Unit

The final set of measurements focused on the power consumption with the SRESLi System Unit using a data logging multimeter as described previously. Figure 25 shows the average power consumption over the night (from 18:00 to 06:00) for one luminaire for one week, with the pedestrian and vehicle detection enabled. We can observe consumption peaks when pedestrian or vehicles are detected and valleys when low activity happens (e.g, between 23:00 and 04:00). Furthermore, the peaks for pedestrians are higher than those for vehicles (of around 90 W at 100% of intensity and 60 W at 50% of intensity, respectively). Since the nominal power consumption of one luminaire is of 665.52 Wh/day in 12 hours operation (see Table 4), the instantaneous power consumption should be of 55.46 W at 100% of intensity. This difference can be explained by initial power required to start the LED electronic driver, which results in a cumulated peak that is higher than the nominal power consumption.

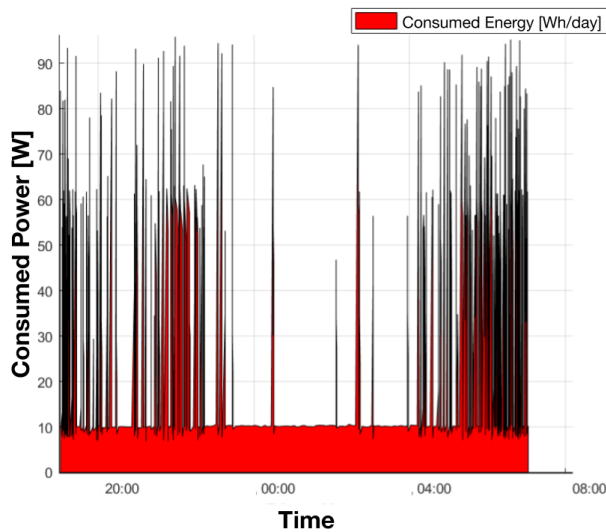


Figure 25: Power consumption for one luminaire throughout the night with SRESLi.

Additionally, at 10% of intensity the power consumption should be of 5.54 W. However, Figure 25 shows that, at this default lowest intensity, the power consumption is close to 10 W. This can be explained by the fact that the light intensity is not linearly proportional to the power consumption, because it is optimized to the maximum of its nominal power. The measured current by the data logging multimeter at 10% of light intensity is of 0.04 A, which corresponds to a power of 8.8 W at 220 VAC (close the 10 W observed in the figure).

Finally, the overall measured power consumption of one luminaire with the SRESLi System Unit throughout the 12 operating hours (i.e., the area under the curve in Figure 25), is of 181 Wh/day. Thus, by comparing this value to the power consumption without any intelligent control system (i.e., 665.52 Wh/day shown in Table 4), we demonstrate an energy saving of 72.8%, thanks to the adaptive lighting and low consumption of the SRESLi System Unit. We therefore can either keep the estimated 100 Wp PV panel (see Section 3.3) to reuse the surplus power (e.g., injecting it to the grid) or we could re-size the PV system to reduce the power peak of the PV panel, thus minimize the cost of the system. These results encourage us for future work on scaling up the SRESLi system, from a pilot towards a widely deployed street lighting system, which may require a more advanced communication protocol, to include monitoring data.

5. CONCLUSIONS

This article describes the design, development, and testing of the Smart Renewable Energy Street Lighting System (SRESLi) as a solution to address the problems related to the traditional street lighting systems. The proposed system was designed with an energy efficiency approach on each stage of the process. Our pilot system shows that the energy savings when using the SRESLi wireless embedded electronic control on a medium- to low-traffic road can be up to 72.8%. Additionally, the SRESLi appears to be an option to provide reliable street lighting for peripheral areas where there is no grid access. Furthermore, surplus power, as a result from energy savings, could be either injected to the grid, in urban areas, or be used for other applications (home lighting, refrigeration, charging mobile devices, and others) in locations with no electrical grid access.

6. ACKNOWLEDGMENTS

This work was partially funded by Universidad Privada Boliviana (Bolivia) and the RETECA Foundation (Switzerland).

7. REFERENCES

- [1] The Royal Society for the Prevention of Accidents, "Road Safety Information - Street Lighting and Road Safety," Edgbaston, Birmingham, 2018.
- [2] R. Beyer and K. Ker, "Street lighting for preventing road traffic injuries," *Cochrane Database Syst. Rev.*, no. 1, pp. 2009–2011, 2009.
- [3] B. Welsh and D. Farrington, "Effects of improved street lighting on crime," *Campbell Syst. Rev.*, vol. 4, no. 13, 2008.
- [4] R. Steinbach, C. Perkins, L. Tompson, S. Johnson, B. Armstrong, J. Green, C. Grundy, P. Wilkinson, and P. Edwards, "The effect of reduced street lighting on road casualties and crime in England and Wales: Controlled interrupted time series analysis," *J. Epidemiol. Community Health*, vol. 69, no. 11, pp. 1118–1124, 2015.
- [5] G. Shahzad, H. Yang, A. W. Ahmad, and C. Lee, "Energy-Efficient Intelligent Street Lighting System Using Traffic-Adaptive Control," *IEEE Sens. J.*, vol. 16, no. 13, pp. 5397–5405, 2016.
- [6] CNDC, "Principales Sistemas Eléctricos," *Reportes Comité Nacional de Despacho de Carga*, 2018. [Online]. Available: <http://www.cndc.bo/sin/index.php>. [Accessed: 12-Jul-2018].
- [7] C. R. B. S. Rodrigues, P. S. O. Almeida, G. M. Soares, J. M. Jorge, D. P. Pinto, and H. A. C. Braga, "An experimental comparison between different technologies arising for public lighting: LED luminaires replacing high pressure sodium lamps," in *Proceedings - ISIE 2011: 2011 IEEE International Symposium on Industrial Electronics*, pp. 141–146, 2011.
- [8] M. Barman, S. Mahapatra, D. Palit, and M. K. Chaudhury, "Energy for Sustainable Development Performance and impact evaluation of solar home lighting systems on the rural livelihood in Assam, India," *Energy Sustain. Dev.*, vol. 38, pp. 10–20, 2017.
- [9] M. Lucano, I. Fuentes, and S. Avilés, "Mapa Solar de Bolivia," 2010. [Online]. Available: http://www.energetica.org.bo/energetica/pdf/publicaciones/mapa_solar.pdf. [Accessed: 07-Feb-2019].
- [10] M. Magno, T. Polonelli, L. Benini, E. Popovici, and S. Member, "A Low Cost , Highly Scalable Wireless Sensor Network Solution to Achieve Smart LED Light Control for Green Buildings," vol. 15, no. 5, pp. 2963–2973, 2015.
- [11] P. C. Veena, P. Tharakan, and H. Haridas, "Smart Street Light System based on Image Processing" in *International Conference on Circuit, Power and Computing Technologies [ICCPCT]*, 2016.

- [12] S. Siregar, "Solar Panel and Battery Street Light Monitoring System Using GSM Wireless Communication System," in *2nd International Conference on Information and Communication Technology (ICoICT)*, pp. 272–275, 2014.
- [13] M. Swati and R. Parekar, "An Intelligent System for Monitoring and Controlling of Street Light using GSM Technology," in *International Conference on Information Processing (ICIP)*, pp. 604–609, 2015.
- [14] A. Kovács, R. Bártai, B. C. Csáji, P. Dudás, B. Háty, G. Pedone, T. Révész, and J. Váncza, "Intelligent control for energy-positive street lighting," *Energy*, vol. 114, pp. 40–51, 2016.
- [15] IEEE Standards Association, *IEEE Standard for Local and metropolitan area networks — Part 15 . 4 : Low-Rate Wireless Personal Area Networks (LR-WPANs)*. New York, US: The Institute of Electrical and Electronics Engineers, Inc., 2011.
- [16] IHS Markit Standards Store, "ANSI TIA/EIA-485-A Electrical Characteristics of Generators and Receivers for Use in Balanced Digital Multipoint Systems." [Online]. Available: https://global.ihs.com/doc_detail.cfm?&document_name=TIA-485 [Accessed: 07-Jan-2019].
- [17] IHS Markit Standards Store, "TSB89 Application Guidelines for TIA/EIA-485." [Online]. Available: https://global.ihs.com/doc_detail.cfm?&item_s_key=00293218 [Accessed: 07-Jan-2018].
- [18] Silicon Labs, "AN0002.1: EFM32 and EFR32 Wireless Gecko Series 1 Hardware Design Considerations," 2016. [Online]. Available: <https://www.silabs.com/documents/public/application-notes/an0002.1-efr32-efm32-series-1-hardware-design-considerations.pdf>. [Accessed: 01-Jun-2017].
- [19] Silicon Labs, "EFR32FG12 Flex Gecko Proprietary Protocol SoC Family Data Sheet," 2016. [Online]. Available: <https://www.silabs.com/documents/public/data-sheets/efr32fg12-datasheet.pdf>. [Accessed: 01-Jun-2017].
- [20] Panasonic, "Infrared array sensor grid-eye." [Online]. Available: <https://industrial.panasonic.com/ww/products/sensors/built-in-sensors/grid-eye>. [Accessed: 06-Mar-2017].
- [21] MaxLinear, "SP3485 - 3.3 V Low Power Half-duplex Rs-485 Transceiver with 10Mbps Data Rate." [Online]. Available: <https://www.maxlinear.com/ds/sp3485.pdf>. [Accessed: 07-Jan-2019].
- [22] Linear Technologies, "LT1762 Series - 150 mA, Low Noise LDO Micropower Regulators," REV A, 2017. [Online]. Available: <http://www.farnell.com/datasheets/42651.pdf>.
- [23] IBNORCA, "NB 1412001:2 Alumbrado público - Reglas generales y especificaciones técnicas." 2013.
- [24] Relux, "ReluxDesktop" [Online]. Available: <https://reluxnet.relux.com/en/relux-desktop.html> [Accessed: 25-Sep-2018].
- [25] A. Alwaeli, M. T. Chaichan, H. A. Kazem, A. M. J. Mahdy, and A. A. Al-waeely, "Optimal Sizing of a Hybrid System of Renewable Energy for Lighting Street in Salalah-Oman using Homer software," *Int. J. Sci. Eng. Appl. Sci.*, vol. 2, no. 5, pp. 157–164, 2016.
- [26] S. Weixiang, "Design of standalone photovoltaic system at minimum cost in Malaysia," in *3rd IEEE Conference on Industrial Electronics and Applications*, no. 3, pp. 702–707, 2008.
- [27] N. D. Kaushika, A. Mishra, and A. K. Rai, *Solar Photovoltaics - Technology, System Design, Reliability and Viability*. Springer International Publishing, 2018.
- [28] LORENTZ, "LC100-M36 High-efficiency PV Module." [Online]. Available: www.lorenz.de. [Accessed: 01-Jul-2018].
- [29] PHOCOS, "Solar Charge Controller CML05-2, CML08-2, CML10-2, CML15-2, CML20 User Manual English," 2011. [Online]. Available: <https://cdn.sos.sk/productdata/ff/87/b1feaf2/cml-05.pdf>. [Accessed: 01-Jun-2018].
- [30] Baterias TOYO, "Bateria TOYO Solar - N70S." [Online]. Available: <http://www.bateriastoyo.com/producto.php?flia=13>. [Accessed: 01-Jul-2018].
- [31] Victron Energy B.V., "Phoenix Inverters (250VA - 1200VA, 230V and 120V, 50Hz or 60Hz)." [Online]. Available: www.victronenergy.com. [Accessed: 01-Jun-2018].
- [32] ON Semiconductor, "BC637, BC639, BC639-16 High Current Transistors." pp. 637–640, 2011.
- [33] R. A. Pastrana Sánchez, "Determinación de cómo el alumbrado de la Ciudad Universitaria afecta la calidad del cielo nocturno del OACS," *Rev. Ciencias Espac.*, vol. 5, no. 1, pp. 6–17, 2012.
- [34] I. O. Mockey Coureaux and E. Millan Alvarez, "Metodología para el Estudio de Instalaciones de Alumbrado Viario," *energética*, vol. XXIV, no. 2, pp. 59–65, 2003.
- [35] T. Markvart, *Solar electricity*, Second Edition, John Wiley & Sons Inc. pp. 95-98, 2000.